Journal of Physics: Conference Series **228** (2010) 012025 doi:10.1088/1742-6596/228/1/012025

Study of three-mode parametric instability

Fengchao Liang[1, 2], Chunnong Zhao[1], Slawomir Gras[1], Li Ju[1], D. G. Blair[1]

[1] School of Physics, University of Western Australia, 35 Stirling Highway, Crawley, Western Australia 6009, Australia
[2] Key Laboratory of Optical System Advanced Manufacturing Technology, Changchun Institute of Optics, Fine Mechanics and Physics, Chinese Academy of Sciences, Changchun 130033, China

E-mail: fcliang@yahoo.cn

Abstract. The effect of parametric instability in advanced interferometric gravitational wave detectors is a potential problem for their proper operation. Great efforts have been made to study the onset of parametric instabilities and to find ways to control them. Here we present an experimental design for studying parametric instability in a 72 m cavity with suspended high quality fused silica mirrors. With 5 W input power and 20 kW circulation power inside the cavity, it is predicted that parametric instability will occur. The resonant condition of parametric instability can be met by thermally tuning the radius of curvature of a test mass. We will present simulation results of parametric gains for different radii of curvature of a test mass. The simulation results will provide the basis for designing the thermal tuning and observation parametric instability experiments. This will provide a test bed for studying parametric instability and its control for next generation detectors.

1. Introduction

Gravitational waves (GW) are a prediction of Einstein's general theory of relativity. The detectable gravitational wave signals on the Earth are extremely small in the order of 10^{-21} in strains. The first-generation ground-based laser interferometers including LIGO in USA [1] and VIRGO in Italy [2] are in operation. LCGT in Japan [3] and AIGO in Australia [4] are future detectors in the plan. The possibility to detect GW signal in the first generation detectors will be rare but it is possible. To increase the sensitivity to certain detection of GW, increasing the power stored in the Fabry-Perot cavity is necessary to reduce the quantum shot noise in addition to other improvements. However, extreme high optical power introduces some unavoidable problems, such as thermal lensing and parametric instabilities [5-7].

Parametric instability in Fabry–Perot cavity is the direct result of opto-acoustic interaction mediated by light radiation pressure force, where high circulating power, low optical and acoustic losses are necessary for high sensitivity, also could lead to the potential instability. If not controlled, parametric instability will cause the test masses' ultrasonic modes to ring at very large amplitudes until saturation [8]. To characterize the effect of the parametric instability, Braginsky et al. [9] obtained a dimensionless parametric gain R. The higher the parametric gain R, the faster a sensitive detector will be disrupted [10].

Various ways to control the instability has been proposed. Zhao et al proposed to thermally tune the radii of curvature (ROC) of a test mass of interferometer arm cavities in order to detune the high order mode resonance and achieve parametric instability suppression [8, 11, 12]. Gras, et al. proposed to use a ring damper (a high loss optical coating on test mass barrel) to reduce the test mass acoustic mode Q-factors with minimal thermal noise degradation [13]. Most recently, the group at MIT proposed to use resonant damper to damp the test mass acoustic modes, which has little effect on the

test mass thermal noise if carefully designed [14]. The group at UWA proposed and demonstrated optical feedback control scheme by injecting an out-of-phase high order mode to destructively interfere with the high order mode inside the cavity.

In this paper, we will present an experimental design of a 72 m high finesse, high *Q*-factor suspended optical cavity for studying parametric instability. In this cavity we expect to observe self-sustained parametric instability by tuning the radius of curvature of a test mass. It will serve as a test bed for studying parametric instability and testing various control schemes. This paper is organized as follows: In the section 2, we will briefly review the theory of parametric instability. In section 3, we will show the configuration of the optical cavity. In section 4, we will show the simulation results of parametric gain as a function of test mass radius of curvature. At the end, we will give brief conclusions.

2. Review of parametric instability theory

In an optical cavity, the thermally driven test mass internal mode vibration will scatter the light incident on the test mass surface into upper and lower sidebands. We define the lower frequency sideband as anti-Stokes mode and the upper frequency sideband as the Stokes mode. Depending on the test mass internal mode shape on the surface, the scattering modes could have high overlap with cavity high order modes. If the scattering sidebands have the same frequencies as the cavity mode frequencies then these sidebands could be resonant inside the cavity and be amplified. The high overlap and the good frequency matching are necessary for the parametric instability.

We know that the frequency of a cavity mode is

$$\omega_{qmn} = \frac{\pi c}{L}\left[q + \frac{(m+n+1)}{\pi}\arccos(\pm\sqrt{g_1 g_2}) \right] \tag{1}$$

So the frequency difference between fundamental mode TEM_{00} (we assume it be Hermite-Gaussian TEM_{00} mode in this paper) and Stokes mode TEM_{mn} is

$$\omega_0 - \omega_s = \frac{\pi c}{L}\left[q_1 - \frac{(m+n)}{\pi}\arccos(\pm\sqrt{g_1 g_2}) \right] \tag{2}$$

and the frequency difference between anti-Stokes mode and the fundamental mode is

$$\omega_{as} - \omega_0 = \frac{\pi c}{L}\left[q_{1a} + \frac{(m+n)}{\pi}\arccos(\pm\sqrt{g_1 g_2}) \right] \tag{3}$$

where q, q_1 and q_{1a} are longitudinal mode indices, m, n are transversal indices, $g_1=1-L/R_1$, $g_2=1-L/R_2$ are g-factors, $\arccos(\pm\sqrt{g_1 g_2})$ is Guoy phase, ω_0 is the frequency of fundamental optical mode, ω_s is the frequency of Stokes mode, ω_{as} is frequency of the anti-Stokes mode, L is the length of the cavity, R_1 and R_2 are the radii of curvature of input test mass (ITM) and end test mass (ETM), respectively.

Braginsky *et al.* [5, 6] have shown that the effective parametric gain R in a simple cavity is given by

$$R = \frac{4PQ_m}{McL\omega_m^2}\left(\frac{Q_1\Lambda_1}{1+(\Delta\omega_1/\delta_1)^2} - \frac{Q_{1a}\Lambda_{1a}}{1+(\Delta\omega_{1a}/\delta_{1a})^2}\right) \tag{4}$$

When the parametric gain R exceeds unity, the acoustic mode will be excited by scattered higher order optical mode. Here P is the circulating power inside the cavity, Q_1 and Q_{1a} are the quality factors of the Stokes and anti-Stokes modes, Q_m is the quality factor of the test mass, $\delta_{1(a)}=\omega_{1(a)}/2Q_{1(a)}$ is relaxation rate, M is the mass of a test mass, $\Delta\omega_1=\omega_0-\omega_s-\omega_m$ and $\Delta\omega_{1a}=\omega_{as}-\omega_0-\omega_m$ are the possible detuning from the ideal resonance case, and Λ_1 and Λ_{1a} are the spatial overlap factors between optical mode shape and acoustic normal mode shape. The overlap factors are defined as

$$\Lambda_1 = \frac{V(\int f_0(\vec{r}_\perp) f_1(\vec{r}_\perp) u_z d\vec{r}_\perp)^2}{\int |f_0|^2 d\vec{r}_\perp \int |f_1|^2 d\vec{r}_\perp \int |\vec{u}|^2 dV}, \quad \Lambda_{1a} = \frac{V(\int f_0(\vec{r}_\perp) f_{1a}(\vec{r}_\perp) u_z d\vec{r}_\perp)^2}{\int |f_0|^2 d\vec{r}_\perp \int |f_{1a}|^2 d\vec{r}_\perp \int |\vec{u}|^2 dV} \tag{5}$$

where f_0 and $f_{1(a)}$ describe the optical field distribution over the mirror surface for the fundamental and Stokes (anti-Stokes) modes, respectively, $\vec{u}$ is the spatial displacement vector for the mechanical mode, u_z is the component of $\vec{u}$ that normal to the mirror surface, the integrals $\int d\vec{r}_\perp$ and $\int dV$

correspond to integration over the mirror surface and the mirror volume, separately. We can see from equation (4) that the parametric gain depends on the frequency detuning, overlapping factors, the *Q*-factors of the test mass acoustic mode and the cavity high order mode. The parametric instability will occur if the parametric gain is greater than unity.

3. Optical cavity design

In order to observe the parametric instability with the laser power that we currently have, we designed an optical cavity that its optical modes have the maximum overlap factor and tunable frequency difference between cavity fundamental mode and the required high order mode to bring them to simultaneous resonance. The second consideration of the design is to use test mass acoustic modes with the simplest mode structure that will simplify the identification of the acoustic mode from the observation.

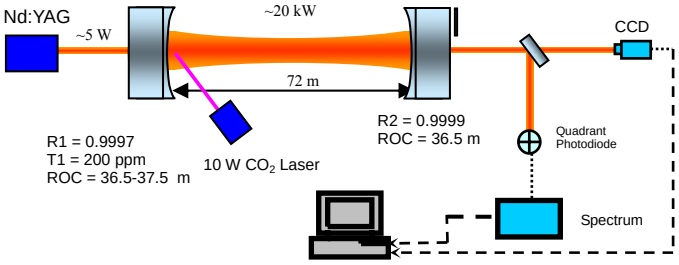

Figure 1. Schematic diagram of three-mode interactions in a simple Fabry-Perot cavity design for parametric instability investigation.

Considering above, we chose the TEM_{01} and the TEM_{10} mode as the candidate optical modes for studying the parametric instability. We will show in the following section that the modes have also large overlap factors with a few test mass acoustic modes from the Finite Element Modeling (FEM). These acoustic mode frequencies are around 155 to 200 kHz. From equation (4), in order to make the scattering mode resonance in the cavity, the frequency difference between TEM_{00} and TEM_{01}/TEM_{10} modes have to be close to the acoustic mode frequency. For the existing vacuum envelope of an optical cavity length ~72 m, we will need the cavity *g*-factors to be ~ 0.95 to match the cavity frequency spacing to the acoustic mode frequencies. In order for these frequencies to be exactly match we will use the CO_2 laser heating the test mass to tune the cavity mode spacing *in situ*.

Table 1. Parameters of optical cavity

	ITM	ETM
Radius of curvature (m)	36.5~37.5	36.5
Material	Fused silica	Fused silica
Reflectivity	0.9997	0.9999
Transmissivity (ppm)	200	<100
Cavity length (m)	72	
Wavelength (μm)	1.064	
Beam waist radius (mm)	10	
Circling power (kw)	20	
Finesse	15000	

The layout of the optical system for investigation of three-mode parametric instability is shown in figure 1. A simple Fabry-Perot optical cavity consists of two fused silica mirrors suspended 72 m apart in a vacuum system. The single-frequency neodymium-doped yttrium aluminum garnet (Nd:YAG) laser is phase locked and mode matched to the TEM_{00} mode of the optical cavity, providing about 5W at the ITM. The nominal finesse of the optical cavity is 15000, giving an

intracavity TEM_{00} power of about 20 kW. With 10 W CO_2 laser thermal tuning of the ROC of ITM, parametric gain R can be changed. If R is greater than 1, parametric instability should occur. Detailed parameters of optical cavity design are showed in table 1.

4. Suspension design and FEM simulation

The test masses will be suspended from the control mass using 25μm niobium ribbon removable modular suspension elements designed by Lee [15]. Such suspension can be removed and exchanged with suspensions of different geometry without the need to change the test mass itself. This will be convenient for us to test the different suspensions. Another advantage is that this method avoids the need for permanent bonding of suspensions to the test mass. Problems associated with bonding, in particular the stresses resulting from the different thermal expansion coefficients of bonded objects, are avoided. Figure 2(a), (b) and (c) show the suspension design of fused silica test mass and a modular suspension peg. To avoid the introduction of thermal noise due to the slip-stick phenomena at the point where the suspension element makes contact with the test mass, it is important that well defined high pressure contact points are created. To achieve this, a 'pin-in-hole' interface has been designed, where pins connected to the suspension element slot into small holes machined into the optic. It is solely the gravitational force acting on the test mass that induces the pressure on the contact points. There are two suspension holes at each flat side of the test mass in an equatorial position. Two holes on each side assure good control of mirror positioning without bonding. Low mechanical loss ribbons and cantilevers suspend the test mass in the vibration isolated vacuum tank. However, the drilled holes will introduce high surface loss since they have not been polished. The high pressure contact between the surface of suspension holes and suspension cantilever could be a source of excess localized loss from friction. These extra losses will lower the Q factor of the test mass. We will simulate this effect of the extra surface loss to the test mass mode Q-factor using FEM and prove that this effect will not stop us to see the parametric instability with designed experimental parameters.

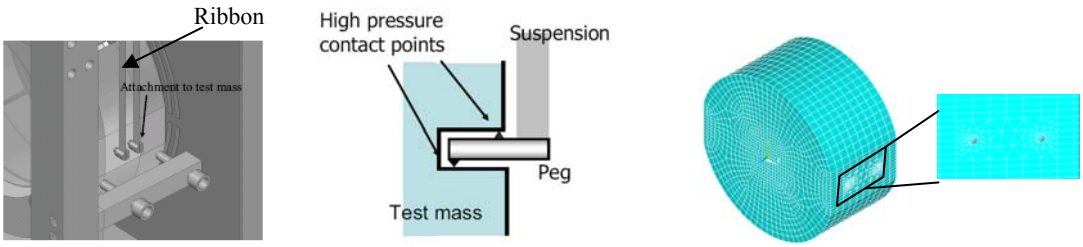

Figure 2. (a) Cantilever-ribbon suspension, (b) suspension peg, (c) Fused silica test mass (Φ100×50) with flats and holes (Φ3 ×4) for cantilever-ribbon suspension.

Figure 2(b) shows the model of a test mass created in the FEM software package, ANSYS®. The dimension of the test mass is 100 mm in diameter and 50 mm in thickness, suspension holes dimension is 3 mm in diameter and 4 mm long. We use Shell93 element to model the high loss holes' surface with the assumption that the surface loss is concentrated on the 100 μm thickness of surface. We use Solid95 element to model the bulk test mass. Test mass material parameters are as follows, Young's modulus is 73 GPa, Poisson ratio is 0.17 and the density is 2202 kg/m^3. After meshing, there are 14505 elements for bulk test mass and holes' surface in the model.

When considering localized loss, the Q factors of the test mass will be different from that of without localized loss, so as the parametric gain R. To include the high surface loss when predicting parametric gain, three types of losses, ϕ_{bulk}, ϕ_{surf} and ϕ_{TM} are defined, where ϕ_{bulk} corresponds to bulk structural loss, ϕ_{surf} associates with the surface loss of the suspension holes, ϕ_{TM} is the total loss of the test mass. Loss angle and Q factors of test mass at different frequency can be calculated by following formulas [16, 17].

$$\phi_{bulk}(f) = 6.5 \times (\frac{S}{V}) + 7.6 \times 10^{-12} \times f^{0.77} \quad (6)$$

$$\phi_{TM} = \phi_{bulk}(f) + \phi_{surf} \times \sum_i E_i / \sum_j E_j \tag{7}$$

$$Q_m(f) = 1/\phi_{TM}(f) \tag{8}$$

where S is the area of test mass, V is the volume of the test mass, f is the frequency, $\sum_i E_i / \sum_j E_j$ is the energy dilution factor depending on the individual mode structure, E_i is strain energy of no. i element of high loss surface of suspension holes, E_j is the strain energy of no. j element of bulk test mass, $Q_m(f)$ is the quality factor of the test mass at frequency f.

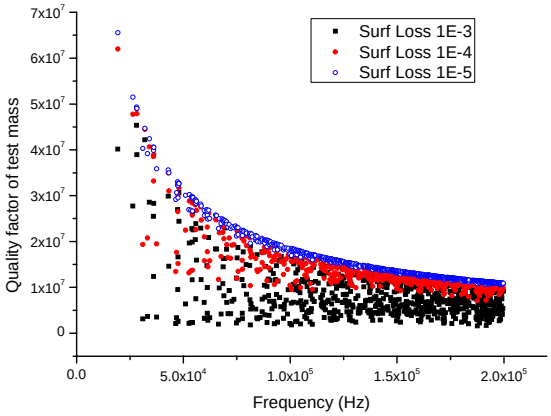

Figure 3. Frequency dependant Q factors of test mass considering different suspension holes' surface loss in the range of 10^{-5} to 10^{-3}.

The resonant frequency and the mode shape of each acoustic mode of the test mass have been obtained using FEM. Q factors of the test mass with the assumption of the holes surface loss in the range of 10^{-5} to 10^{-3} are shown in figure 3. It can be seen from figure 3 that Q factors decrease along with the increasing of the frequency because the fused silica's mechanical loss is frequency depended. The Q factors decrease with increased suspension hole surface losses and the changes depend on the mode frequency because the different mode shape has different coupling effect to the suspension holes' surfaces. This agrees with ideas of test mass barrel coating for suppressing parametric instability with the minimum thermal noise penalty [13].

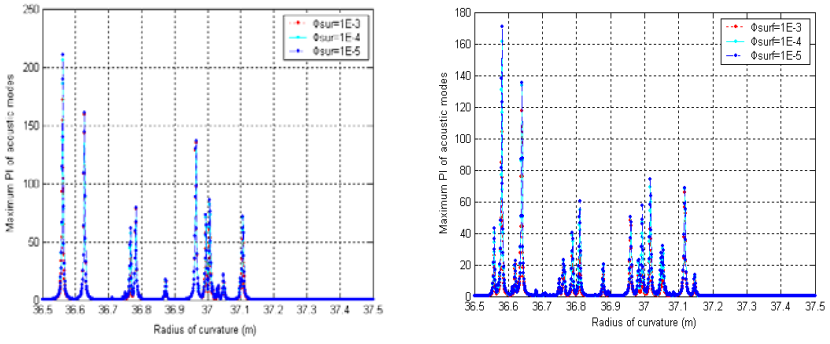

Figure 4. Maximum parametric gain vs. ROC of ITM (a) for TEM_{01}; (b) for TEM_{10}.

To match the cavity mode spacing to the test mass acoustic mode frequencies and then to obtain the maximum parametric gain, a CO_2 laser will be used to thermally tune the ROC of the ITM from 36.5 to 37.5 m, which will scan through various cavity mode spacing and then various parametric gain peaks. In order to obtain high precision of parametric instability gain in the simulation, a step of 1 mm is selected for tuning the ROC of ITM in the simulation. During this tuning course, Gouy phase for

the optical cavity ranges from 2.81 to 2.91 radian, and the frequency distance between fundamental optical mode and Stokes mode, ω_0–ω_s, ranges from 155 kHz to 219 kHz. So test mass' acoustic modes with resonant frequency within this range should be able to get small detuning when interacting with the other two optical modes. If there is also a great overlapping factor between the acoustic mode shape and Stokes mode shape, the parametric gain may be greater than unity and parametric oscillation instability may occur. So when evaluating parametric gain, we put emphasis on acoustic modes with resonant frequency between 155 kHz to 200 kHz.

We calculated the parametric gain for each acoustic mode as a function of ROC of ITM for the designed optical cavity. Our analysis assumes that the fundamental optical mode is TEM_{00} mode and higher order mode is TEM_{01} and TEM_{10}. Acoustic modes are modeled using ANSYS® finite element modeling package with 14505 meshing elements. The fundamental optical mode and Stokes mode, the overlapping factors and parametric gains are evaluated in MATLAB®. Figure 4 shows the maximum parametric gain of each acoustic mode versus the ROC of the ITM. Figure 4 (a) is for TEM_{01} mode (b) is for TEM_{10} mode while including the suspension holes' high surface loss. It can be seen from figure 4 that a little change of ROC of the ITM can result in dramatic change of parametric gain value. There are more than 10 acoustic modes that could interact with the other two optical modes result in parametric instability, i.e., the acoustic modes can scatter TEM_{00} into TEM_{01} or TEM_{10} mode with small detuning and high overlap factors. But through tuning the ROC of ITM, parametric gain can be suppressed much lower until less than 1. So in principle, thermally tuning of ROC of ITM can scan through the maximum parametric gain regime that will be used to investigate parametric instability effect. Two typical instable modes examples and their relative parameters are showed in figure 5.

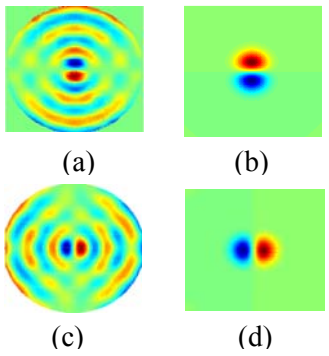

Figure 5. Typical acoustic and optical mode shapes, (a) ROC = 37.107 m, ω_m=196.69 kHz, Λ = 2.1608, R = 60.891 m, $\Delta\omega_1$=31.844 Hz, Q_m= 9.377×10^7, Φ_{surf} = 10^{-3}; (b) the field distribution of the cavity TEM_{01} mode showing high overlap of the acoustic mode and optical mode structures; (c) ROC = 37.118 m, ω_m = 197.35 kHz, Λ = 2.0864, R = 65.672 m, $\Delta\omega_1$ = 37.509Hz, Q_m=10.551×10^7, Φ_{surf} = 10^{-3}; (d) the field distribution of the TEM_{10} showing high overlap of the acoustic mode and optical mode structures.

5. Conclusion

We presented an experimental design of a 72 m high finesse, high Q-factor suspended optical cavity for studying parametric instability. By tuning the ROC of the ITM the simulation shows that there are about 10 potentially unstable acoustic modes in the frequency range of 155 to 200 kHz with parametric gains between 1 and 250 if the test mass mechanical Q-factor ~1 to 7×10^7. Even if the actual test mass Q-factor is ~10^6 we can still see some modes of parametric gain greater than unity.

This experimental setup will serve as a test bed for studying parametric instability and testing various control schemes.

Acknowledgment

This is a project of Australian Consortium for Gravitational Astronomy, supported by Australian Research Council and Western Australia government research centre of excellence scheme.

References

[1] Abramovici, et al., Science 256 (1992) 325.
[2] F. Acernese, et al., Class. Quantum Grav. 23 (2006) S635.
[3] K. Kuroda, Class. Quantum Grav. 23 (2006) S215.
[4] D.E. McClelland, et al., Class. Quantum Grav. 23 (2006) S41.
[5] V.B. Braginsky, S.E. Strigin, S.P. Vyatchanin, Phys. Lett. A287, 331, (2001).
[6] V.B. Braginsky, S.E. Strigin, S.P. Vyatchanin, Phys. Lett. A305, 111, (2002).

[7] W. Kells and E. D'Ambrosio, Phys. Lett. A299, 326, (2002).
[8] L. Ju, C. Zhao, S. Gras, J. Degallaix, D.G. Blair, et al., Phys. Lett. A 355 (2006) 419.
[9] V. B. Braginsky and S. P. Vyatchanin, Phys. Lett. A 293, 228, (2002).
[10] D.E. McClelland, et al., Class. Quantum Grav. 23 (2006) S41.
[11] C. Zhao, L. Ju, J. Degallaix, S. Gras, D.G. Blair, Phys. Rev. Lett. 94 (2005) 121102.
[12] L. Ju, S. Gras, C. Zhao, J. Degallaix, D.G. Blair, Phys. Lett. A 354 (2006) 360.
[13] S. Gras, D.G. Blair, L. Ju. Physics Letters A 372 (2008) 1348–1356.
[14] Evans M et al.. 2008 LSC/Virgo Collaboration Meeting, LIGO-G080541-00-Z.
[15] B. Lee, Advanced test mass suspensions and electrostatic control for AIGO, PhD thesis, University of Western Australia, 2007.
[16] S.D. Penn, A. Ageev, D. Busby, G.M. Harry, et al., Physics Letters A 352 (2006) 3–6.
[17] Gregory M Harry, Andri M Gretarsson, et al., Class. Quantum Grav. 19 (2002) 897–917.